


Expression of B7-H3 and TIM-3 in gastric-type endocervical adenocarcinoma: prevalence, association with PD-L1 expression, and prognostic significance

Yao Sun^{1†}, Xin Zhou^{1,2†}, Elena Lucas^{3,4}, Lili Chen⁵, Huijuan Zhang^{2*}, Hao Chen^{3,4*} and Feng Zhou^{1,2*} 

¹Department of Pathology, Zhejiang University School of Medicine Women's Hospital, Hangzhou, Zhejiang Province, PR China

²Department of Pathology, International Peace Maternity and Child Health Hospital Affiliated to Shanghai Jiao Tong University School of Medicine, Shanghai, PR China

³Department of Pathology, University of Texas Southwestern Medical Center, Dallas, TX, USA

⁴Department of Pathology, Parkland Hospital, Dallas, TX, USA

⁵Department of Gynecology, Zhejiang University School of Medicine Women's Hospital, Hangzhou, Zhejiang Province, PR China

*Correspondence to: Feng Zhou, Department of Pathology, Women's Hospital, School of Medicine, Zhejiang University, Hangzhou, Zhejiang Province 310006, PR China and Department of Pathology, International Peace Maternity and Child Health Hospital Affiliated to Shanghai Jiao Tong University School of Medicine, Shanghai 200030, PR China. E-mail: fungchew@zju.edu.cn; Hao Chen, Department of Pathology, University of Texas Southwestern Medical Center, 5323 Harry Hines Boulevard, Dallas, TX 75390, USA. E-mail: hao.chen@utsouthwestern.edu; Huijuan Zhang, Department of Pathology, International Peace Maternity and Child Health Hospital Affiliated to Shanghai Jiao Tong University School of Medicine, Shanghai 200030, PR China. E-mail: zhanghj815@sjtu.edu.cn

†These authors contributed equally to this work.

Abstract

Gastric-type endocervical adenocarcinoma (GEA) is the second most common subtype of endocervical adenocarcinoma and has a poor prognosis. Anti-programmed death-1 and anti-programmed death-ligand 1 (PD-L1) inhibitors have emerged as a major treatment option for GEA; however, data on the expression of other immune checkpoints in GEA are limited. We analyzed the expression of T-cell immunoglobulin and mucin-domain containing-3 (TIM-3) and B7 homolog 3 protein (B7-H3) in 58 GEA and investigated their prognostic significance as well as association with PD-L1 expression and other known prognostic factors. Applying the tumor proportion score (TPS) with a cutoff of 1%, B7-H3 and TIM-3 were present in 48.3% and 17.2% of cases, respectively. Applying the combined positive score (CPS) with a cutoff of 1, TIM-3 expression was present in 70.7% of cases. Moreover, the expression of three checkpoints (B7-H3, TIM-3, and PD-L1) was incompletely overlapping. Patients with B7-H3 positive tumors (by TPS) or TIM-3 positive tumors (by TPS) had significantly worse recurrence-free survival (RFS) and overall survival (OS) (log-rank). Using CPS, patients with TIM-3 positive tumors showed significantly worse RFS (log-rank). Similarly, B7-H3 positivity (by TPS) and TIM-3 positivity (by TPS) were associated with worse RFS and OS in univariate analysis. TIM-3 positivity (by CPS) was associated with worse RFS in univariate analysis and the final Cox multivariate analysis. In conclusion, our results show that (1) B7-H3 and TIM-3 are frequently expressed in GEA and their expression overlaps incompletely with PD-L1; and (2) both B7-H3 and TIM-3 are independent negative prognostic markers in GEA.

Keywords: gastric-type endocervical adenocarcinoma; immune checkpoint; B7-H3; TIM-3; prognosis

Received 25 July 2023; Revised 23 August 2023; Accepted 3 September 2023

No conflicts of interest were declared.

Introduction

As the second most common subtype of endocervical adenocarcinoma (ECA) and the most common subtype of HPV independent (HPVI) ECA, gastric-type endocervical adenocarcinoma (GEA) accounts for 10–15% of all ECAs worldwide and up

to 25% in Asian countries [1–5]. Compared with HPV-associated ECA, GEA has higher prevalence of destructive invasion, extrauterine spread, and advanced stage at presentation [1,5]. GEA is also associated with poor response to chemoradiation treatment [6,7] and significantly worse disease-free and overall survival [1,5,8,9].

© 2023 The Authors. *The Journal of Pathology: Clinical Research* published by The Pathological Society of Great Britain and Ireland and John Wiley & Sons Ltd.

This is an open access article under the terms of the [Creative Commons Attribution-NonCommercial-NoDerivs](https://creativecommons.org/licenses/by-nc-nd/4.0/) License, which permits use and distribution in any medium, provided the original work is properly cited, the use is non-commercial and no modifications or adaptations are made.

The tumor microenvironment plays a crucial role in tumor immune surveillance and tumor cells may evade immune surveillance through upregulation of expression of immune checkpoint signaling molecules [10,11]. Blocking immune checkpoints using immune checkpoint inhibitors (ICI), such as anti-programmed death-1 (PD-1) and anti-programmed death-ligand 1 (PD-L1) inhibitors, has emerged as a major treatment in cervical cancers [12–14]. While anti-PD-1 and anti-PD-L1 inhibitors often lead to more durable responses than chemotherapy [15], the relatively low response rate in most cancers and acquired resistance to ICI remain the major roadblocks [15,16]. Mechanisms of resistance or non-responsiveness to ICI remain poorly understood, but evidence suggests multifactorial causes, including tumor mutational burden [17], PD-L1 expression level [18], interferon- γ signaling pathways [19], and inactivation of antigen presentation [20]. Interestingly, the upregulation of alternative immune checkpoints has also been shown to contribute to the resistance to anti-PD-1 and anti-PD-L1 inhibitor therapy [21,22]. Synergy of anti-tumor effect from combination of ICIs has been previously reported [23,24]. For these reasons, characterization of various immune checkpoints in tumors remains the forefront of current efforts to search for immunotherapeutic targets [21,25,26]. Among alternative checkpoints, two have been shown to be attractive and promising targets for cancer immunotherapy [27,28]. T-cell immunoglobulin and mucin-domain containing-3 (TIM-3) is an immunosuppressive protein that enhances tolerance and inhibits anti-tumor immunity [29–31]. TIM-3 is expressed by various immune cells and upregulated in various cancers [32]. B7 homolog 3 protein (B7-H3) is another checkpoint that is frequently upregulated in many malignant tumors and participates in tumor microenvironment shaping and development [28,33].

In addition to the potentially predictive value for targeted immunotherapies, the prognostic significance of immune checkpoints has gained attention lately. This study was designed to investigate the prevalence and prognostic significance of B7-H3 and TIM-3 expression, their correlation with PD-L1 expression, and association with clinical parameters in GEA.

Materials and methods

Case selection

The study was conducted with the approval from the institutional review board at Women's Hospital, School of Medicine, Zhejiang University, PR China. A total of

58 cases of GEA accessioned between January 2014 and December 2021 were selected, all of which were also included in our previous study of PD-L1 and HER2 expression in GEA [34]. Patients' clinicopathological information including age, clinical stage, follow-up, and clinical outcome were extracted from the electronic clinical information system database of Women's Hospital. H&E-stained slides were reviewed by two gynecologic pathologists (YS and FZ) in a blinded fashion and the pathologic diagnosis was confirmed. All tumors were classified according to the 2020 WHO Classification of Female Genital Tumors [34].

Immunohistochemistry

Immunohistochemistry was performed on whole tissue sections of formalin-fixed, paraffin-embedded tumor tissue according to the previously published protocol [35]. Positively charged slides with tissue sections cut at 4- μ m thickness were dried in an oven for 1 h at 56–60 °C. Deparaffinization, rehydration, and target retrieval were performed in a three-in-one procedure, per the manufacturer's instructions, by fully submerging the slides in preheated (65 °C) EnVision™ FLEX Target Retrieval Solution at high pH (9.0) (Dako/Agilent, Santa Clara, CA, USA) for B7-H3, TIM-3, and CD8, and incubating slides at 97 °C for 20 min. After incubation, the slides were removed from the solution and immediately immersed in room temperature wash buffer for 5 min. Afterwards, the slides were placed in the Autostainer Link 48 platform (Dako/Agilent) and FLEX peroxidase blocking was performed for 5 min, and then incubated with primary antibodies. The following primary antibodies and dilutions were used: monoclonal rabbit B7-H3 (clone D9M2L, 1:150 dilution, Cell Signaling Technology, Danvers, MA, USA), monoclonal rabbit TIM-3 (clone D5D5R, 1:100 dilution, Cell Signaling Technology), and monoclonal mouse CD8 (clone C8/144B, RTU, Dako/Agilent). Incubation time with primary antibody was 60 min for B7-H3 and, 35 min for TIM-3, and 20 min for CD8. Subsequently, all slides were rinsed in wash buffer for 5 min, and then incubated with the EnVision™ FLEX HRP visualization reagent for 30 min at room temperature. After rinsing in wash buffer for 5 min, the enzymatic conversion of the subsequently added 3,3'-diaminobenzidine (DAB) tetrahydrochloride chromogen was performed for 10 min at room temperature. Slides were subsequently counterstained for 5 min with hematoxylin (Link, Dako/Agilent), and finally mounted using nonaqueous permanent mounting media.

Assessment of B7-H3 and TIM-3 expression

As there are no established criteria for assessment of B7-H3 or TIM-3, the same scoring systems and positivity thresholds as FDA-approved methods for PD-L1 assessment were used in other solid tumors [12] and recently in endometrial serous carcinoma [35].

Two scoring methods, tumor proportion score (TPS) and combined positive score (CPS), were used in the current study. TPS was calculated as the percentage of tumor cells with membranous B7-H3 or TIM-3 expression. CPS was calculated as the number of B7-H3 or TIM-3-staining cells (tumor cells, lymphocytes, and macrophages) divided by the total number of viable tumor cells, multiplied by 100 and truncated to 100 if >100. Both scores ranged from 0 to 100. For both markers, a cutoff score $\geq 1\%$ for TPS and ≥ 1 for CPS were used to define positivity and additional cutoffs (e.g. 10 and 20) were used to further analyze the significance of marker expression. In the CPS system, for scoring of mononuclear immune cells (lymphocytes and macrophages), only intratumoral and peritumoral (within one $\times 20$ field from the tumor nest edge) immune cells were enumerated. Stromal immune cells distant from the tumor were excluded.

Image analysis and calculation of CD8+ tumor infiltrating lymphocyte density

Whole slide images of CD8 immunostained slides were generated for image analysis by Aperio ScanScope AT Turbo Scanner (Leica Biosystems, Heidelberg, Germany). Quantification of total tumor area and percentage of positive staining cells was performed using the open source QuPath software (v0.3.2) (<https://qupath.github.io>). Areas for quantification were annotated using QuPath analysis tools. The percentage of CD8 staining was determined using the color-deconvolution tool. CD8+ tumor infiltrating lymphocyte (TIL) density was calculated as total CD8+ cells divided by the area comprising the intratumor and areas in direct contact with the tumor periphery (mm^2). CD8+ TIL density was dichotomized into two groups (low and high) based on the optimal cutoff value obtained through consideration of tumor recurrence using receiver operating characteristic (ROC) curve analysis. The optimal cutoff value was obtained using the Youden index, which maximizes the vertical distance from the reference line.

Statistical analysis

Two-tailed chi square tests were used to determine the association between categorical variables, such as correlation of CD8+ TIL density groups with

expression of different immune checkpoints. Cohen's Kappa (κ) was used to measure the agreement between different immune checkpoints. Overall survival (OS) was defined as the time interval from the date of pathological diagnosis to the date of death from any cause or last follow-up, and recurrence-free survival (RFS) was the time interval from the date of surgery to the date of the first recurrence. Survival curves were plotted by the Kaplan–Meier method, and log-rank tests were used to compare OS and RFS among various patient groups. Univariate and multivariate Cox regression models were used to identify significant predictors associated with clinical outcomes. To avoid statistical bias caused by insufficient sample size, only variables with a p value less than 0.2 in the univariate model were included in the multivariate analysis. GraphPad Prism 9.0 software (San Diego, CA, USA) was used for survival analysis, while other statistical analyses were performed using IBM SPSS 25.0 (Armonk, NY, USA) software, and all p values < 0.05 were considered statistically significant.

Ethics approval and consent to participate

This study was approved by the ethics committee of the Zhejiang University School of Medicine Women's Hospital (IRB-20230238-R).

Results

Patient characteristics

A total of 58 cases of GEA were included in the current study, including 51 hysterectomies, 3 cone excisions, and 4 loop electrosurgical excision procedure excisions. Among the 58 patients, 56 were clinically staged using the International Federation of Gynecology and Obstetrics (FIGO) 2018 system [36] based on available histologic and radiological information. Fifty-seven of 58 patients had complete follow-up information available. The median age was 46.5 years, ranging from 25 to 77 years. Fifty-one hysterectomy specimens were available for analyzing pathological risk factors, including deep stromal invasion, lymphovascular invasion (LVI), and lymph node metastasis (LNM). FIGO stage I-IIA tumors were considered low-stage tumors, and FIGO stage IIB-IV tumors were considered as advanced stage tumors. More than 50% stromal invasion of the full thickness of cervix was considered as deep stromal invasion. Patient demographics, pathologic diagnoses, clinical stage, and follow-up information are summarized in Table 1.

Table 1. Clinicopathological information of GEA patients

Age (years)	Median 46.5, range 25–77	
Clinicopathological parameter	<i>n</i>	%
Stage (FIGO)		
I-IIA	36	62.1
IIB-IV	20	34.5
NA	2	3.4
Deep stromal invasion		
Yes	43	74.1
No	8	13.8
NA	7	12.1
Lymph node metastasis		
Yes	19	32.8
No	32	55.2
NA	7	12.1
Lymphovascular invasion		
Yes	25	43.1
No	26	44.8
NA	7	12.1
Radiotherapy/chemotherapy		
Yes	50	86.2
No	7	12.1
NA	1	1.7

NA, not available.

B7-H3 and TIM-3 expression in GEA and their association with clinicopathological parameters

In GEA cases, B7-H3 was expressed exclusively in tumor cells, and showed predominantly patchy and occasionally diffuse distribution. When cutoff $\geq 1\%$ (by TPS) was used, 48.3% (28/58) cases were B7-H3 positive, of which 17 were ‘1–10%’, 6 were ‘10–20%’, and 5 were ‘>20%’. TIM-3 was expressed predominantly on the surface of immune cells, and focally of tumor cells. The spatial distribution was predominantly patchy, focal, or multifocal with accentuation at the tumor edge and tumor-stroma interface. When cutoff $\geq 1\%$ (by TPS) was used, 17.2% (10/58) cases were TIM-3 positive, all of which were ‘1–10%’. When cutoff ≥ 1 (by CPS) was used, 70.7% (41/58) cases were TIM-3 positive, 23 were ‘1–10’, 14 were ‘10–20’, and 4 were ‘>20’. Representative images of the expression of B7-H3 and TIM-3 are shown in Figure 1A.

The association between the expression of B7-H3 and TIM-3, and patients’ clinicopathological parameters are shown in supplementary material, Table S1. As illustrated in Figure 2A, TIM-3 positivity (by CPS) was associated with increased risk of deep stromal invasion ($p < 0.0001$). As illustrated in Figure 2B, B7-H3 positivity (by TPS) and TIM-3 positivity (by TPS) were associated with an increased risk of LNM ($p = 0.012$ and $p = 0.043$, respectively). B7-H3 positivity (by TPS) was associated with increased risk of LVI ($p = 0.036$) (Figure 2C).

In addition, we investigated the association among the expression of B7-H3, TIM-3, and PD-L1. Data for PD-L1 expression were derived from our previous study [34], with 37.9% (22/58) of cases being positive by TPS and 75.9% (44/58) of cases being positive by CPS. Patterns of expression of the three markers are presented in a case matrix in Figure 1B. Regarding the concordance between the three immune checkpoints, when using TPS, 81.8% (18/22) of PD-L1 positive cases were also positive for B7-H3 or TIM-3, while 36% (13/36) of PD-L1 negative cases were positive for B7-H3 or TIM-3. When using CPS, 88.6% (39/44) of PD-L1 positive cases were also positive for B7-H3 or TIM-3, while 50% (7/14) of PD-L1 negative cases were positive for B7-H3 or TIM-3. Overall, 60.3% (35/58) of GEAs were positive for at least one of the three checkpoints when TPS was used, while 87.9% (51/58) of GEAs positive for at least one of the three checkpoints when CPS was used. All pairwise associations were then formally investigated among the three observations by κ statistics. Moderate positive association was found between PD-L1 positivity (by TPS) and B7-H3 positivity (by TPS) ($\kappa = 0.444$, $p = 0.001$), and between PD-L1 positivity (by CPS) and TIM-3 positivity (by CPS) ($\kappa = 0.430$, $p = 0.003$). PD-L1 positivity (by CPS) and B7-H3 positivity (by TPS) had fair positive association ($\kappa = 0.255$, $p = 0.021$). Correlation between B7-H3, TIM-3, and PD-L1 positivity in GEA is summarized in Table 2.

Correlation of immune checkpoint expression with CD8+ TIL density

As illustrated in Figure 3A, the density of CD8+ TILs varied among tumors (median 195 cells/mm², range 39–1,236 cells/mm²). Based on TIL density and the optimal cutoff value determined by ROC curve analysis, tumors were divided into CD8+ low (<262 cells/mm²) and CD8+ high (≥ 262 cells/mm²) groups.

The CD8+ high group accounted for 41.4% (24/58) of all GEA cases (Figure 3C), while CD8+ low group accounted for 58.6% (34/58). The percentage of the expression of three markers in CD8+ low or high groups is presented in Figure 3D. Using TPS, PD-L1 positivity was significantly higher in CD8+ high GEAs than in CD8+ low GEAs (62.5% versus 20.6%, $p = 0.001$). Similarly, using CPS, PD-L1 positivity was significantly higher in CD8+ high GEAs than in CD8+ low GEAs (91.7% versus 64.7%, $p = 0.018$). Regardless of scoring system, no significant difference in the expression of B7-H3 (using TPS: $p = 0.198$) or TIM-3 (using TPS: $p = 0.798$; using CPS: $p = 0.076$) was found between CD8+ low and high groups.

Table 2. Correlation between B7-H3, TIM-3, and PD-L1 in GEA

Variables	B7-H3 (TPS)		TIM-3 (TPS)		TIM-3 (CPS)		PD-L1 (TPS)	
	Negative	Positive	Negative	Positive	Negative	Positive	Negative	Positive
TIM-3 (TPS)	$\rho = 0.245, \kappa = 0.153$							
Negative	27	21						
Positive	3	7						
TIM-3 (CPS)	$\rho = 0.064, \kappa = 0.218$		$\rho = 0.063, \kappa = 0.159$					
Negative	12	5	17	0				
Positive	18	23	31	10				
PD-L1 (TPS)	$\rho = 0.001^*, \kappa = 0.444$		$\rho = 0.221, \kappa = 0.181$		$\rho = 0.146, \kappa = 0.154$			
Negative	25	11	32	4	13	23		
Positive	5	17	16	6	4	18		
PD-L1 (CPS)	$\rho = 0.021, \kappa = 0.255$		$\rho = 0.458, \kappa = 0.073$		$\rho = 0.003^*, \kappa = 0.430$		$\rho = 0.001^*, \kappa = 0.326$	
Negative	11	3	13	1	9	8	14	0
Positive	19	25	35	9	5	36	22	22

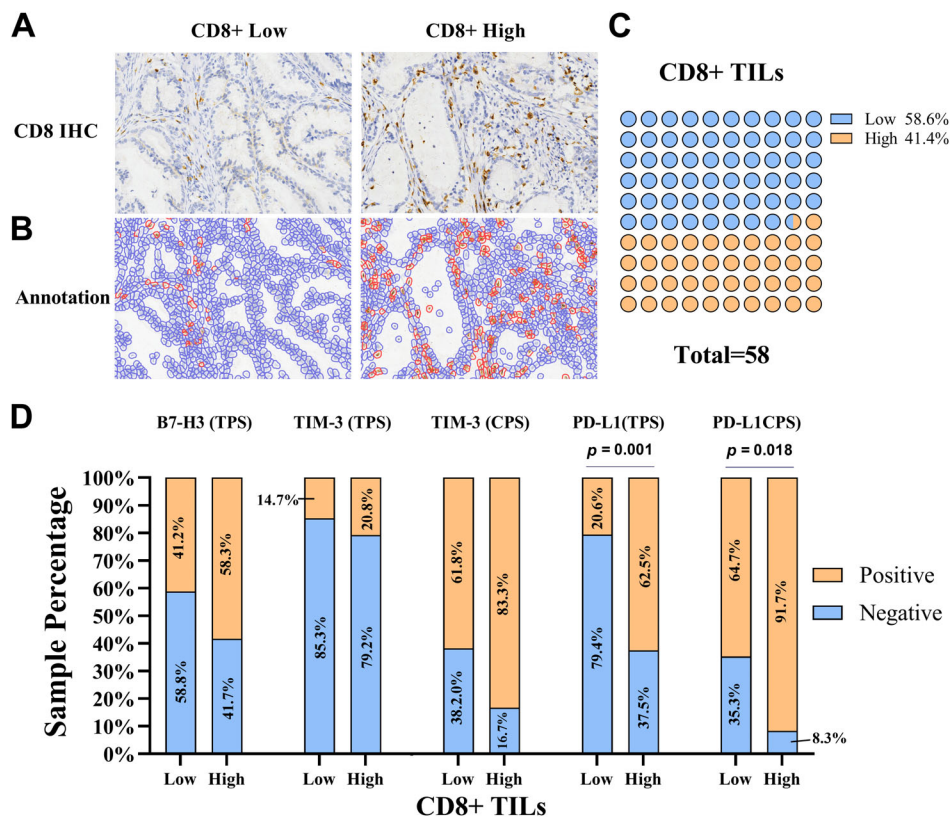
* $p < 0.05$.

Figure 3. CD8+ TIL density and its correlation with B7-H3, TIM-3, and PD-L1 expression. (A) CD8 IHC and (B) corresponding image annotation of CD8+ TILs using the Aperio image analysis tool: CD8+ lymphocytes are annotated in red; other unstained cells are in blue. (C) Case percentage matrix arranged according to CD8+ TIL density. (D) Correlation of CD8+ TIL density with B7-H3, TIM-3, and PD-L1 expression.

with B7-H3 positive tumors (by TPS) had significantly worse RFS and OS ($p = 0.004$ and $p = 0.003$, respectively). Similarly, patients with TIM-3 positive tumors (by TPS) also had significantly worse RFS and OS ($p = 0.009$ and $p = 0.007$,

respectively). In contrast, patients with TIM-3 positive tumors (by CPS) showed significantly worse RFS ($p = 0.017$) and no significant difference in OS ($p = 0.110$). As the expression of B7-H3 and TIM-3 in the majority of cases was low (TPS: 1–10% or

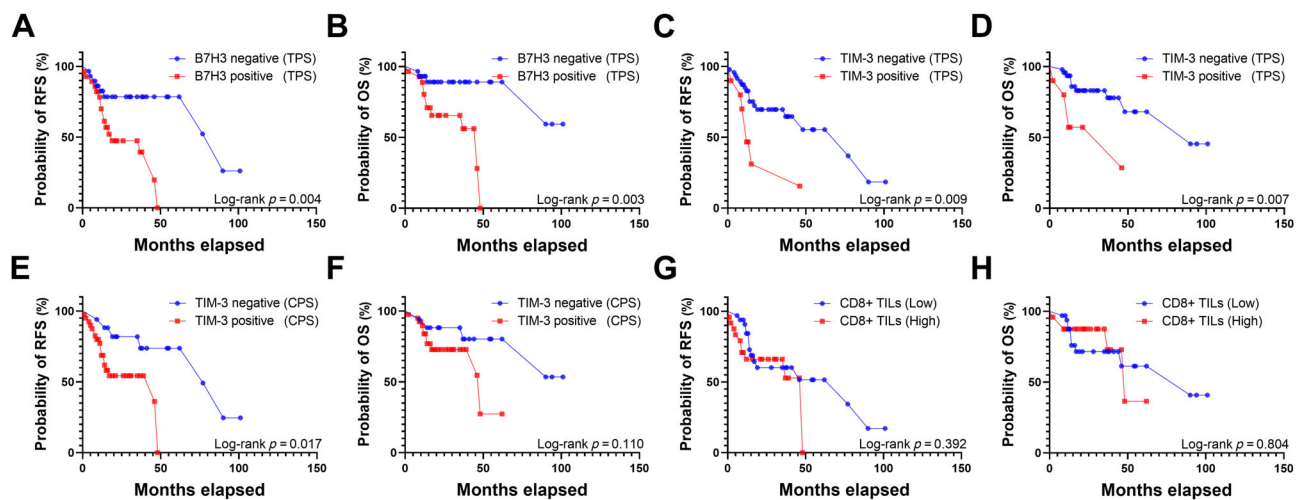


Figure 4. Survival analysis of B7-H3, TIM-3, and CD8+ TIL density. (A,B) Kaplan–Meier curves of RFS and OS for patients with B7-H3 positivity in tumor cells (red) and B7-H3 negativity in tumor cells (blue): (A) RFS; (B) OS. (C,D) Kaplan–Meier curves of RFS and OS for patients with TIM-3 positivity (red) and TIM-3 negativity (blue) using TPS (cutoff 1%): (C) RFS; (D) OS. (E,F) Kaplan–Meier curves of RFS and OS for patients with TIM-3 positivity (red) and TIM-3 negativity (blue) using CPS (cutoff 1): (E) RFS; (F) OS. (G,H), Kaplan–Meier curves of RFS and OS for patients in the low CD8+ TIL density group (red) and the high CD8+ TIL density group (blue): (G) RFS; (H) OS.

Table 3. Correlation of pathological risk factors with outcome in GEA

Variable	Category	Events (n)	Median RFS (months)	HR	95% CI	p value	Median OS (months)	HR	95% CI	p value
B7-H3 (TPS)	Positive	28	19.00	3.080	1.358 to 6.984	0.004*	46.00	4.486	1.581 to 12.720	0.003
	Negative	29	90.00				Undefined			
TIM-3 (TPS)	Positive	10	12.00	2.992	0.877 to 10.200	0.009*	46.00	3.832	0.786 to 18.680	0.007*
	Negative	47	77.00				90.00			
TIM-3 (CPS)	Positive	40	46.00	2.663	1.195 to 5.936	0.017*	48.00	2.288	0.828 to 6.323	0.110
	Negative	17	77.00				Undefined			
CD8	Low	33	77.00	1.402	0.602 to 3.267	0.392	90.00	0.878	0.306 to 2.514	0.804
	High	24	48.00				48.00			
DSI	Positive	43	46.00	4.536	1.493 to 13.780	0.100	48.00	-	-1.000 to -1.000	0.101
	Negative	8	Undefined				Undefined			
LNM	Positive	19	15.00	3.103	1.218 to 7.905	0.008*	46.00	2.440	0.753 to 7.904	0.112
	Negative	32	Undefined				Undefined			
LVI	Positive	26	19.00	3.350	1.374 to 8.164	0.006*	46.00	4.960	1.543 to 15.940	0.005
	Negative	25	90.00				90.00			
Age	<46.5	20	Undefined	2.207	0.991 to 4.917	0.055	Undefined	1.641	0.599 to 4.536	0.337
	≥46.5	37	19.00				90			
Clinical stage	High	20	17.00	2.765	1.151 to 6.641	0.010*	46.00	2.132	0.693 to 6.558	0.139
	Low	36	77.00				Undefined			

Clinical stage low: FIGO I-IIa; clinical stage high: FIGO IIb-IV.

DSI, deep stromal invasion; HR, hazard ratio.

**p* < 0.05.

CPS: 1–10), we were not able to perform statistical analysis between ‘low’ and ‘high’ expression groups by other cutoff points (e.g. TPS: 10% or 20%; CPS: 10 or 20).

As shown in supplementary material, Table S2, B7-H3 (by TPS) and TIM-3 (by TPS or CPS) were associated with worse RFS in univariate analysis (*p* = 0.007 for B7-H3; *p* = 0.013 and *p* = 0.025 for

TIM-3 by TPS and CPS respectively). B7-H3 (by TPS) and TIM-3 (by TPS) were also associated with worse OS in univariate analysis (*p* = 0.008 and *p* = 0.013 respectively). Moreover, univariate analysis also showed that poorer RFS correlated with other known prognostic factors such as advanced stage (*p* = 0.014), LNM (*p* = 0.012), and LVI (*p* = 0.011). LVI correlated with poorer OS in patients with GEA

($p = 0.014$). Variables with $p < 0.2$ in the univariate analysis were then evaluated in multivariate analysis using stepwise selection. As shown in supplementary material, Table S3, age ≥ 46.5 years ($p = 0.024$) and TIM-3 positivity by CPS ($p = 0.043$) were associated with worse RFS in the final Cox multivariate analysis, while advanced stage was found to be associated with worse OS ($p = 0.039$). In contrast, CD8+ TIL density demonstrated no prognostic significance in either univariate or multivariate analysis.

Discussion

The purpose of this study was to investigate the expression of B7-H3 and TIM-3 in a large cohort of GEA, their prognostic value, and association with PD-L1, CD8+ TILs, and prognostic clinical parameters. We found high prevalence of B7-H3 and TIM-3 expression in GEA. B7-H3 was exclusively expressed by tumor cells, while TIM-3 was predominantly expressed by immune cells. The expression of three checkpoints (B7-H3, TIM-3, and PD-L1) was incompletely overlapping. Unlike PD-L1 expression, the expression of B7-H3 and TIM-3 was not associated with CD8+ TIL density. Furthermore, the expression of B7-H3 and TIM-3 was associated with more aggressive clinical behavior and worse prognosis.

B7-H3 is a member of the B7 family of cell surface molecules, which can inhibit the activation and function of T-cells [37], and serves as a negative regulator in T-cell-mediated immune responses to convey protection of tumor cells from immune attack [38]. TIM-3 plays a key role in inhibiting Th1 responses and the production of cytokines such as tumor necrosis factor and interferon- γ [39]. B7-H3 and TIM-3 expression in solid tumors is predominantly associated with worse prognosis in various cancers [40–42]. Only few studies have investigated the prevalence of B7-H3 and TIM-3 expression and their prognostic significance in cervical cancers. Huang *et al* studied 108 cervical cancers [including 98 squamous cell carcinomas (SCCs) and 10 ECA] and found B7-H3 expression in 72% of cases and its inverse association with OS [43]. Han *et al* investigated 100 cervical SCC and found B7-H3 expression in 62% cases and its inverse association with disease-free survival [44]. Li *et al* studied 90 cervical SCC and reported B7-H3 expression in 72% cases and strong expression was associated with worse prognosis [45]. The above three studies used *H*-score (or a range 39–1,236 cells/mm² modified version of it) to evaluate B7-H3 positivity. Zhang *et al*

reported B7-H3 expression in 552 cervical cancers (including 406 SCCs and 146 ECA), in which TPS $\geq 5\%$ cutoff was used to define B7-H3 positivity [46]. In this study, B7-H3 positivity was found in 36% SCC and 21.2% ECA. In addition, B7-H3 expression was associated with worse recurrence-free and overall survival. In their cohort of 673 cervical cancers (including 491 SCCs and 115 ECA), with TPS $\geq 5\%$ cutoff for positivity, Zong *et al* found B7-H3 expression in 62.8% cases and failed to demonstrate its prognostic significance [47]. In their study of 50 cervical clear cell carcinomas, another rare type of HPV ECA, Zong *et al* reported B7-H3 expression in 16% cases (TPS $\geq 5\%$ positivity cutoff) [48]. Although there were variations in reported prevalence of B7-H3 expression among these studies, likely due to the difference in methodology and variation in included tumor types, high prevalence and association with worse prognosis were found in the majority of the reports. In our study, we found B7-H3 expression was 48.3% by TPS and TIM-3 expression was 17.2% by TPS and 70.7% by CPS. We could not directly compare our results to those of prior studies on cervical carcinoma, however, because of the difference in methodologies and histologic tumor types.

Our data show that the distribution of the expression of three checkpoints shows some, but incomplete, overlap. Moderate positive association ($\kappa = 0.444$ and $p = 0.001$) was found between PD-L1 and B7-H3 positivity (by TPS), and between PD-L1 and TIM-3 positivity (by CPS) ($\kappa = 0.430$ and $p = 0.003$). PD-L1 positivity (by CPS) and B7-H3 positivity (by TPS) had fair positive association ($\kappa = 0.255$, $p = 0.021$). While the majority of PD-L1 positive GEAs were also positive for B7-H3 or TIM-3, a significant proportion of PD-L1-negative GEAs were also positive for B7-H3 or TIM-3. This observation may have significant clinical implications in that (1) B7-H3 and TIM-3 may be promising therapeutic targets in PD-L1 negative tumors, or in PD-L1 positive tumors that develop resistance to anti-PD-L1 inhibitor; (2) combination of ICIs may have a synergistic anti-tumor effect and potentially decrease the likelihood of developing resistance to single ICI treatment. An increasing number of drugs targeting TIM-3 are currently being developed, such as, for example, MBG453, TQB2618, Sym023, and AZD7789. These drugs are also being clinically tested for their efficacy and safety, both individually and in combination with PD-1/PD-L1 antibody therapies, across various advanced solid tumors. A phase I/II clinical trial evaluating the efficacy of sabatolimab (MBG453) either as a monotherapy or in combination with spartalizumab (an anti-PD-1 antibody) in

patients with various advanced solid tumors has demonstrated favorable tolerability and preliminary signs of anti-tumor activity when these two drugs are used in combination [49]. Clinical trials of TIM-3 targeted therapies in a variety of solid tumors are currently underway with great momentum; however, specific clinical trials for cervical cancer have not yet been conducted [50–52]. More importantly, future clinical trials that are multicenter, well designed, and have large sample size are needed to explore the efficacy and safety of TIM-3 targeted therapies in cervical cancer, particularly in patients with gastric-type cervical adenocarcinoma.

Increased CD8+ T-cell infiltration is generally considered as an independent positive prognostic indicator in solid tumors [53]. Additionally, tumors may develop various strategies to evade anti-tumor immune surveillance, including the increased expression of immune checkpoints. A parallel increase in CD8+ TILs and PD-L1 expression has been observed in various solid tumor types [54,55] including Müllerian cancers such as ovarian cancer [56,57], endometrial cancers [35,58,59], and cervical cancers [60,61]. A similar parallel increase between CD8+ TILs and PD-L1 expression in GEAs was found in the current study, suggesting the upregulation of PD-L1 as an adaptive immune resistance mechanism developed by tumor cells to avert destruction by TILs [62,63]. Conversely, no significant association with CD8+ TILs was found for the B7-H3 or TIM-3 expression in GEA. Our previous studies have demonstrated the frequent PD-L1 expression in ECA with PD-L1 being a negative prognostic marker, suggestive of the predictive and prognostic role of PD-L1 in this tumor group [34,64]. Unlike PD-L1, studies on TIM-3 and B7-H3 expression in cervical cancers are limited and mainly focused on SCC or unselected cohorts of cervical cancer [44–47,65,66]. The results of these studies demonstrated predominantly negative association between survival and the expression of TIM-3 and B7-H3. Information regarding TIM-3 and B7-H3 in ECA, especially in GEA, is largely lacking. In this study, we found that B7-H3 and TIM-3 are independent negative prognostic markers associated with more aggressive behavior and worse survival in GEAs.

In summary, our results show that the expression of B7-H3 and TIM-3 in GEAs is frequent. Both B7-H3 and TIM-3 are independent negative prognostic markers in GEAs. Our data provide insight into the complexity of the tumor microenvironment and suggest that B7-H3 and TIM-3 may be potential therapeutic targets in GEA. Our study cohort was relatively small due to the rarity of this entity. As a future

direction, investigation of these markers on larger, potentially multicenter patient cohorts would be needed to validate our findings. As none of the patients included in this study received any anti-PD-L1 inhibitor treatment, it would be of interest to investigate the expression of B7-H3 and TIM-3 in post-anti-PD-L1 treated tumors, especially in tumors with resistance to treatment.

Author contributions statement

FZ had full access to all of the data in the study, and takes responsibility for the integrity of the data and accuracy of the data analysis. YS, XZ, EL and LC were involved in drafting the manuscript and revising it critically for important intellectual content. HZ and HC reviewed and edited the manuscript. All authors read and approved the final manuscript. All researchers listed as authors are independent from the funders, and all final decisions about the research were made without constraint by the investigators.

Data availability statement

The datasets generated during and/or analysed during the current study are available from the corresponding author.

References

1. Karamurzin YS, Kiyokawa T, Parkash V, *et al.* Gastric-type endocervical adenocarcinoma: an aggressive tumor with unusual metastatic patterns and poor prognosis. *Am J Surg Pathol* 2015; **39**: 1449–1457.
2. Kusanagi Y, Kojima A, Mikami Y, *et al.* Absence of high-risk human papillomavirus (HPV) detection in endocervical adenocarcinoma with gastric morphology and phenotype. *Am J Pathol* 2010; **177**: 2169–2175.
3. Park SB, Moon MH, Hong SR, *et al.* Adenoma malignum of the uterine cervix: ultrasonographic findings in 11 patients. *Ultrasound Obstet Gynecol* 2011; **38**: 716–721.
4. Stolnicu S, Barsan I, Hoang L, *et al.* International Endocervical Adenocarcinoma Criteria and Classification (IECC): a new pathogenetic classification for invasive adenocarcinomas of the endocervix. *Am J Surg Pathol* 2018; **42**: 214–226.
5. Kojima A, Mikami Y, Sudo T, *et al.* Gastric morphology and immunophenotype predict poor outcome in mucinous adenocarcinoma of the uterine cervix. *Am J Surg Pathol* 2007; **31**: 664–672.
6. Kuruma A, Kodama M, Hori Y, *et al.* Gastric-type adenocarcinoma of the uterine cervix associated with poor response to definitive radiotherapy. *Cancers (Basel)* 2022; **15**: 170.

7. Kojima A, Shimada M, Mikami Y, et al. Chemoresistance of gastric-type mucinous carcinoma of the uterine cervix: a study of the Sankai Gynecology Study Group. *Int J Gynecol Cancer* 2018; **28**: 99–106.
8. Nishio S, Mikami Y, Tokunaga H, et al. Analysis of gastric-type mucinous carcinoma of the uterine cervix – an aggressive tumor with a poor prognosis: a multi-institutional study. *Gynecol Oncol* 2019; **153**: 13–19.
9. Ehmman S, Sassine D, Straubhar AM, et al. Gastric-type adenocarcinoma of the cervix: clinical outcomes and genomic drivers. *Gynecol Oncol* 2022; **167**: 458–466.
10. Keir ME, Butte MJ, Freeman GJ, et al. PD-1 and its ligands in tolerance and immunity. *Annu Rev Immunol* 2008; **26**: 677–704.
11. Pardoll DM. The blockade of immune checkpoints in cancer immunotherapy. *Nat Rev Cancer* 2012; **12**: 252–264.
12. Davis AA, Patel VG. The role of PD-L1 expression as a predictive biomarker: an analysis of all US Food and Drug Administration (FDA) approvals of immune checkpoint inhibitors. *J Immunother Cancer* 2019; **7**: 278.
13. Frenel JS, Le Tourneau C, O'Neil B, et al. Safety and efficacy of pembrolizumab in advanced, programmed death ligand 1-positive cervical cancer: results from the phase Ib KEYNOTE-028 trial. *J Clin Oncol* 2017; **35**: 4035–4041.
14. Chung HC, Ros W, Delord JP, et al. Efficacy and safety of pembrolizumab in previously treated advanced cervical cancer: results from the phase II KEYNOTE-158 study. *J Clin Oncol* 2019; **37**: 1470–1478.
15. Ribas A, Wolchok JD. Cancer immunotherapy using checkpoint blockade. *Science* 2018; **359**: 1350–1355.
16. He X, Xu C. Immune checkpoint signaling and cancer immunotherapy. *Cell Res* 2020; **30**: 660–669.
17. Samstein RM, Lee CH, Shoushtari AN, et al. Tumor mutational load predicts survival after immunotherapy across multiple cancer types. *Nat Genet* 2019; **51**: 202–206.
18. Topalian SL, Hodi FS, Brahmer JR, et al. Safety, activity, and immune correlates of anti-PD-1 antibody in cancer. *N Engl J Med* 2012; **366**: 2443–2454.
19. Gao J, Shi LZ, Zhao H, et al. Loss of IFN- γ pathway genes in tumor cells as a mechanism of resistance to anti-CTLA-4 therapy. *Cell* 2016; **167**: 397–404.e399.
20. Sade-Feldman M, Jiao YJ, Chen JH, et al. Resistance to checkpoint blockade therapy through inactivation of antigen presentation. *Nat Commun* 2017; **8**: 1136.
21. Koyama S, Akbay EA, Li YY, et al. Adaptive resistance to therapeutic PD-1 blockade is associated with upregulation of alternative immune checkpoints. *Nat Commun* 2016; **7**: 10501.
22. Huang L, Xu Y, Fang J, et al. Targeting STAT3 abrogates Tim-3 upregulation of adaptive resistance to PD-1 blockade on regulatory T cells of melanoma. *Front Immunol* 2021; **12**: 654749.
23. Sun F, Guo ZS, Gregory AD, et al. Dual but not single PD-1 or TIM-3 blockade enhances oncolytic virotherapy in refractory lung cancer. *J Immunother Cancer* 2020; **8**: e000294.
24. Ju F, Luo Y, Lin C, et al. Oncolytic virus expressing PD-1 inhibitors activates a collaborative intratumoral immune response to control tumor and synergizes with CTLA-4 or TIM-3 blockade. *J Immunother Cancer* 2022; **10**: e004762.
25. Hellmann MD, Friedman CF, Wolchok JD. Combinatorial cancer immunotherapies. *Adv Immunol* 2016; **130**: 251–277.
26. Dempke WCM, Fenchel K, Uciechowski P, et al. Second- and third-generation drugs for immuno-oncology treatment – the more the better? *Eur J Cancer* 2017; **74**: 55–72.
27. Tian T, Li Z. Targeting Tim-3 in cancer with resistance to PD-1/PD-L1 blockade. *Front Oncol* 2021; **11**: 731175.
28. Zhou WT, Jin WL. B7-H3/CD276: an emerging cancer immunotherapy. *Front Immunol* 2021; **12**: 701006.
29. Anderson AC, Anderson DE, Bregoli L, et al. Promotion of tissue inflammation by the immune receptor Tim-3 expressed on innate immune cells. *Science* 2007; **318**: 1141–1143.
30. Hastings WD, Anderson DE, Kassam N, et al. TIM-3 is expressed on activated human CD4+ T cells and regulates Th1 and Th17 cytokines. *Eur J Immunol* 2009; **39**: 2492–2501.
31. Monney L, Sabatos CA, Gaglia JL, et al. Th1-specific cell surface protein Tim-3 regulates macrophage activation and severity of an autoimmune disease. *Nature* 2002; **415**: 536–541.
32. Qin S, Dong B, Yi M, et al. Prognostic values of TIM-3 expression in patients with solid tumors: a meta-analysis and database evaluation. *Front Oncol* 2020; **10**: 1288.
33. Liu S, Liang J, Liu Z, et al. The role of CD276 in cancers. *Front Oncol* 2021; **11**: 654684.
34. Wang S, Zhou X, Niu S, et al. Assessment of HER2 in gastric-type endocervical adenocarcinoma and its prognostic significance. *Mod Pathol* 2023; **36**: 100148.
35. Chen H, Molberg K, Carrick K, et al. Prevalence and prognostic significance of PD-L1, TIM-3 and B7-H3 expression in endometrial serous carcinoma. *Mod Pathol* 2022; **35**: 1955–1965.
36. Bhatla N, Aoki D, Sharma DN, et al. Cancer of the cervix uteri. *Int J Gynaecol Obstet* 2018; **143**: 22–36.
37. Prasad DV, Nguyen T, Li Z, et al. Murine B7-H3 is a negative regulator of T cells. *J Immunol* 2004; **173**: 2500–2506.
38. Suh WK, Gajewska BU, Okada H, et al. The B7 family member B7-H3 preferentially down-regulates T helper type 1-mediated immune responses. *Nat Immunol* 2003; **4**: 899–906.
39. Das M, Zhu C, Kuchroo VK. Tim-3 and its role in regulating anti-tumor immunity. *Immunol Rev* 2017; **276**: 97–111.
40. Zang K, Hui L, Wang M, et al. TIM-3 as a prognostic marker and a potential immunotherapy target in human malignant tumors: a meta-analysis and bioinformatics validation. *Front Oncol* 2021; **11**: 579351.
41. Liu C, Zhang G, Xiang K, et al. Targeting the immune checkpoint B7-H3 for next-generation cancer immunotherapy. *Cancer Immunol Immunother* 2021; **71**: 1549–1567.
42. Loos M, Hedderich DM, Friess H, et al. B7-h3 and its role in antitumor immunity. *Clin Dev Immunol* 2010; **2010**: 683875.
43. Huang C, Zhou L, Chang X, et al. B7-H3, B7-H4, Foxp3 and IL-2 expression in cervical cancer: associations with patient outcome and clinical significance. *Oncol Rep* 2016; **35**: 2183–2190.
44. Han S, Shi X, Liu L, et al. Roles of B7-H3 in cervical cancer and its prognostic value. *J Cancer* 2018; **9**: 2612–2624.
45. Li Y, Zhang J, Han S, et al. B7-H3 promotes the proliferation, migration and invasiveness of cervical cancer cells and is an indicator of poor prognosis. *Oncol Rep* 2017; **38**: 1043–1050.

46. Zhang Q, Zong L, Zhang H, *et al.* Expression of B7-H3 correlates with PD-L1 and poor prognosis in patients with cervical cancer. *Onco Targets Ther* 2021; **14**: 4275–4283.
47. Zong L, Gu Y, Zhou Y, *et al.* Expression of B7 family checkpoint proteins in cervical cancer. *Mod Pathol* 2022; **35**: 786–793.
48. Zong L, Zhang Q, Zhou Y, *et al.* Expression and significance of immune checkpoints in clear cell carcinoma of the uterine cervix. *J Immunol Res* 2020; **2020**: 1283632.
49. Curigliano G, Gelderblom H, Mach N, *et al.* Phase I/IIb clinical trial of sabatolimab, an anti-TIM-3 antibody, alone and in combination with spartalizumab, an anti-PD-1 antibody, in advanced solid tumors. *Clin Cancer Res* 2021; **27**: 3620–3629.
50. Lakhani N. Sym021 in Combination With Either Sym022 or Sym023 or Sym023 and Irinotecan in Patients With Recurrent Advanced Selected Solid Tumor Malignancies 2023. [Accessed 25 August 2023]. Available from: <https://clinicaltrials.gov/study/NCT04641871?cond=NCT04641871&rank=1>
51. A Study to Assess the Safety and Efficacy of AZD7789 in Participants With Advanced or Metastatic Solid Cancer 2023. [Accessed 25 August 2023]. Available from: <https://clinicaltrials.gov/study/NCT04931654?cond=NCT04931654&rank=1>
52. A Study to Assess the Safety and Efficacy of LB1410 in Participants With Advanced Solid Tumor or Lymphoma(Keyplus-001) 2023. [Accessed 25 August 2023]. Available from: <https://clinicaltrials.gov/study/NCT05357651?cond=NCT05357651&rank=1>
53. Fridman WH, Pagès F, Sautès-Fridman C, *et al.* The immune contexture in human tumours: impact on clinical outcome. *Nat Rev Cancer* 2012; **12**: 298–306.
54. Herbst RS, Soria JC, Kowanetz M, *et al.* Predictive correlates of response to the anti-PD-L1 antibody MPDL3280A in cancer patients. *Nature* 2014; **515**: 563–567.
55. Tumeh PC, Harview CL, Yearley JH, *et al.* PD-1 blockade induces responses by inhibiting adaptive immune resistance. *Nature* 2014; **515**: 568–571.
56. Chen H, Molberg K, Strickland AL, *et al.* PD-L1 expression and CD8+ tumor-infiltrating lymphocytes in different types of tubo-ovarian carcinoma and their prognostic value in high-grade serous carcinoma. *Am J Surg Pathol* 2020; **44**: 1050–1060.
57. Zhang T, Zhou X, Zhang X, *et al.* Discordance of PD-L1 expression in primary and metastatic ovarian high-grade serous carcinoma and its correlation with CD8+ tumor-infiltrating lymphocytes and patient prognosis. *Virchows Arch* 2023; **482**: 755–766.
58. Zong L, Sun Z, Mo S, *et al.* PD-L1 expression in tumor cells is associated with a favorable prognosis in patients with high-risk endometrial cancer. *Gynecol Oncol* 2021; **162**: 631–637.
59. Vagios S, Yiannou P, Giannikaki E, *et al.* The impact of programmed cell death-ligand 1 (PD-L1) and CD8 expression in grade 3 endometrial carcinomas. *Int J Clin Oncol* 2019; **24**: 1419–1428.
60. Mezache L, Paniccia B, Nyinawabera A, *et al.* Enhanced expression of PD L1 in cervical intraepithelial neoplasia and cervical cancers. *Mod Pathol* 2015; **28**: 1594–1602.
61. Rivera-Colon G, Chen H, Molberg K, *et al.* PD-L1 expression in endocervical adenocarcinoma: correlation with patterns of tumor invasion, CD8+ tumor-infiltrating lymphocytes, and clinical outcomes. *Am J Surg Pathol* 2021; **45**: 742–752.
62. Taube JM, Anders RA, Young GD, *et al.* Colocalization of inflammatory response with B7-h1 expression in human melanocytic lesions supports an adaptive resistance mechanism of immune escape. *Sci Transl Med* 2012; **4**: 127ra137.
63. Teng MW, Ngiow SF, Ribas A, *et al.* Classifying cancers based on T-cell infiltration and PD-L1. *Cancer Res* 2015; **75**: 2139–2145.
64. Chen L, Lucas E, Zhang X, *et al.* Programmed death-ligand 1 expression in human papillomavirus-independent cervical adenocarcinoma and its prognostic significance. *Histopathology* 2022; **80**: 338–347.
65. Curley J, Conaway MR, Chinn Z, *et al.* Looking past PD-L1: expression of immune checkpoint TIM-3 and its ligand galectin-9 in cervical and vulvar squamous neoplasia. *Mod Pathol* 2020; **33**: 1182–1192.
66. Cao Y, Zhou X, Huang X, *et al.* Tim-3 expression in cervical cancer promotes tumor metastasis. *PLoS One* 2013; **8**: e53834.

SUPPLEMENTARY MATERIAL ONLINE

Table S1. Expression of B7-H3, TIM-3, and their association with clinicopathologic parameters of patients with GEA

Table S2. Univariate analysis of RFS and OS among patients with GEA

Table S3. Multivariate analysis of RFS and OS among patients with GEA